UPPSALA
UNIVERSITET

*Digital Comprehensive Summaries of Uppsala Dissertations from the Faculty of Science and Technology* 1587

# Metallicity determination of M dwarfs

SARA LINDGREN



ACTA
UNIVERSITATIS
UPSALIENSIS
UPPSALA
2017

ISSN 1651-6214
ISBN 978-91-513-0127-3
urn:nbn:se:uu:diva-332102

Dissertation presented at Uppsala University to be publicly examined in Polhemssalen, Ångströmslaboratoriet, Lägerhyddsvägen 1, Uppsala, Tuesday, 12 December 2017 at 09:30 for the degree of Doctor of Philosophy. The examination will be conducted in English. Faculty examiner: Professor Ansgar Reiners (Georg-August-Universität Göttingen, Institut für Astrophysik).

**Abstract**
Lindgren, S. 2017. Metallicity determination of M dwarfs. *Digital Comprehensive Summaries of Uppsala Dissertations from the Faculty of Science and Technology* 1587. 46 pp. Uppsala: Acta Universitatis Upsaliensis. ISBN 978-91-513-0127-3.

M dwarfs constitute around 70% of all stars in the local Galaxy. Their multitude together with their long main-sequence lifetimes make them important for studies of global properties of the Galaxy such as the initial mass function or the structure and kinematics of stellar populations. In addition, the exoplanet community is showing an increasing interest for those small, cold stars. However, very few M dwarfs are well characterized, and in the case of exoplanetary systems the stellar parameters have a direct influence on the derived planet properties.

Stellar parameters of M dwarfs are difficult to determine because of their low surface temperatures that result in an optical spectrum dominated by molecular lines. Most previous works have therefore relied on empirical calibrations. High-resolution spectrographs operating in the infrared, a wavelength region less affected by molecular lines, have recently opened up a new window for the investigation of M dwarfs. In the two first papers of this thesis we have shown that we can determine the metallicity, and in some cases the effective temperature, using synthetic spectral fitting with improved accuracy.

This method is time consuming and therefore not practical or even feasible for studies of large samples of M dwarfs. When comparing our results from the high-resolution studies with available photometric calibrations we find systematic differences. In the third paper we therefore used our sample to determine a new photometric metallicity calibration. Compared to previous calibrations our new photometric calibration shows improved statistical characteristics, and our calibration gives similar results as spectroscopic calibrations. In a comparison with theoretical calculations we find a good agreement of the shapes and slopes of iso-metallicity lines with our empirical relation. Applying the photometric calibration to a sample of M dwarfs with confirmed exoplanets we find a possible giant planet-metallicity correlation for M dwarfs.

*Keywords:* stars: low mass - stars: abundances, fundamental parameters - technique: spectroscopic, photometric - planets and satellites: formation

*Sara Lindgren, Department of Physics and Astronomy, Observational Astronomy, 516, Uppsala University, SE-751 20 Uppsala, Sweden.*



ISSN 1651-6214
ISBN 978-91-513-0127-3
urn:nbn:se:uu:diva-332102 (http://urn.kb.se/resolve?urn=urn:nbn:se:uu:diva-332102)

*To my husky*

# List of papers

This thesis is based on the following papers, which are referred to in the text by their Roman numerals.

I **Lindgren, S.**, Heiter, U., and Seifahrt, A. (2016)
*Metallicity determination of M dwarfs. High-resolution IR spectroscopy*
A&A, **597**, A100

II **Lindgren, S.** and Heiter, U. (2017)
*Metallicity determination of M dwarfs. Expanded parameter range in metallicity and effective temperature*
A&A, **604**, A97

III **Lindgren, S.**, Heiter, U., Edvardsson, B., and Liljegren, S. (2017)
*A photometic calibration of M dwarfs based on high-resolution infrared spectroscopy*
To be submitted to A&A

# List of papers not included in the thesis

The following are publications to which I have contributed as author, but that are not included in this thesis.

1. **Lindgren, S.**, Gelino, C., Martin, E., Tinney, C., Schneider, A., Kirkpatrick, D., Cushing, M., Beichman, C., and Faherty, J., (2017)
   *Looking for close, faint companions among the coldest brown dwarfs*
   To be submitted to ApJ

# Contents

# 1. Stellar classification

With a few exceptions within our own Solar System, all current knowledge of astronomical objects is based on studies of emitted or scattered light from different parts of the electromagnetic spectrum.[1] The history of modern spectroscopy began in the seventeenth century when Isaac Newton used a prism to refract white light into a rainbow of colors, something Newton referred to as a spectrum. In 1802 the English chemist and physicist William Wollaston was the first to discover spectral lines in the solar spectrum. A few years later in 1814, the German optician Joseph von Fraunhofer looked at both the Sun and the redder star Betelgeuse and realized that the pattern of dark lines in the spectra was different between the two astronomical objects. These mysterious dark lines became known as the Fraunhofer lines.

The next important step was taken in 1859 when the German physicist Gustav Kirchhoff formulated the so-called Kirchhoff's laws describing the difference between continuous, emission and absorption spectra. Later, together with the German chemist Robert Bunsen, Kirchhoff realized that several of the Fraunhofer lines in the stellar spectra were consistent with the observed emission lines of heated chemical elements. However, the physical explanation behind the formation of spectral lines was not discovered until the twentieth century with the development of quantum mechanics by mathematicians and physicists such as Max Planck, Ernest Rutherford, Niels Bohr, Louis de Broglie, Erwin Schördinger, Albert Einstein, and many more.

That different type of stars show variation of their spectral features has been known since Fraunhofer's observations of the Sun and Betelgeuse, and became increasingly apparent with the first large surveys of stars in the late nineteenth century. The Italian astronomer Angelo Secchi pioneered stellar classification by introducing three classes of stars in the 1860s: white and blue stars with broad hydrogen lines, yellow stars with less strong hydrogen lines and evident metallic lines, and orange and red stars with complex spectra. In the mid 1880s one of the more influential photographic surveys led by Edward C. Pickering began at the Harvard College Observatory, a survey that continued for nearly four decades. This resulted in the Henry Draper catalogue, today containing well over 350,000 classified stars.

In 1901 Annie Cannon used these data to introduce the today familiar O B A F G K M stellar classification, where O is the hottest type and M the coldest. Later in the 1920s, the British-American astronomer Cecilia Payne-Gaposchkin used the Saha equation to show that the spectral sequence was due

[1] Except neutrinos, cosmic rays and gravitational waves.

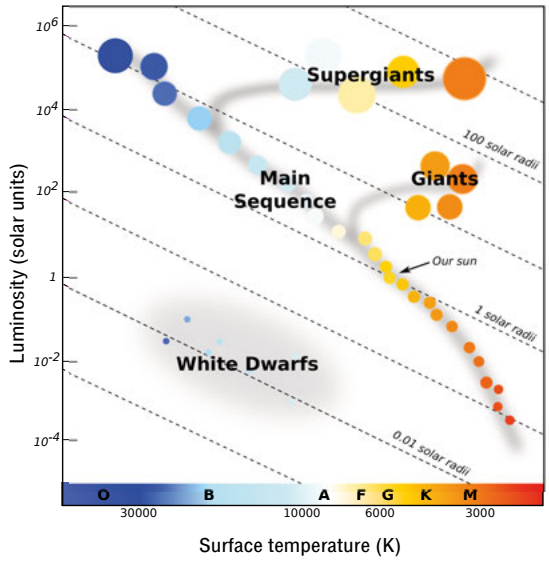


*Figure 1.1.* An example of a Hertzsprung-Russell diagram. Luminosity is shown on the y-axis and the surface temperature on the x-axis, both on a logarithmic scale. The dashed lines indicate stars with the same radii, starting from 1000 solar radii on the top right, down to 0.001 solar radii on the bottom left.

to an underlying temperature sequence. Today we know that the stellar mass is the underlying parameter governing this temperature sequence for dwarfs.

A couple of years earlier, in 1911, the Danish engineer and amateur astronomer Ejnar Hertzsprung had analyzed the stars in the Pleiades and Hyades clusters and realized that the stars with colder spectral types were divided into two distinct luminosity groups. He refereed to the brighter stars as giants. The American astronomer Henry Russell independently discovered the same thing Hertzsprung, and in 1914 he published the first diagram showing different stars' observed absolute magnitude versus their spectral type. This type of plot is today known as a Hertzsprung-Russell diagram, where a schematic version is shown in Fig. 1.1. As Hertzsprung, Russell refereed to the more luminous stars as giants and termed their colder counterpart dwarfs. This naming convention is natural as Stefan-Boltzmann law gives that two stars with the same temperature (indicated by the same spectral type) the more luminous star have a larger radius.

Modern astronomy uses the Morgan-Keenan spectral classification from 1943, developed by the two American astronomers William Morgan and Philip Keenan. Stars are classified both according to their temperature and luminosity (surface gravity), differentiating between evolutionary stages by roman numerals. For example, giants are denoted with III and dwarfs with V. In addition to the spectral classes of normal stars: O B A F G K M, each class is divided into ten sub-classes, 0 being the hottest and 9 the coldest. Typical ranges of

**Table 1.1.** *Approximate parameter ranges for the different spectral classes for main-sequence stars according to the Morgan-Keenan classification.*

| Class | $T_{\text{eff}}$ (K) | Mass ($M_\odot$) | Radius ($R_\odot$) | Luminosity ($L_\odot$) |
|---|---|---|---|---|
| O | $> 30\,000$ | $> 16$ | $> 6.6$ | $> 50\,000$ |
| B | 10 000-30 000 | 2.1-16 | 1.8-6.6 | 100-50 000 |
| A | 7500-10 000 | 1.4-2.1 | 1.4-1.8 | 5-100 |
| F | 6000-7500 | 1.04-1.4 | 1.15-1.4 | 1.5-5 |
| G | 5200-6000 | 0.8-1.04 | 0.96-1.15 | 0.6-1.5 |
| K | 4000-5200 | 0.5-0.8 | 0.7-0.96 | 0.08-0.6 |
| M | 2700-4000 | 0.08-0.5 | $< 0.7$ | $< 0.08$ |

temperature, mass, radius and luminosity for dwarfs in each spectral class are shown in Table. 1.1.

Stars spend most of their life-times as dwarfs, populating the main-sequence. During this evolutionary phase stars are powered by hydrogen fusion in their core, and a hydrostatic equilibrium exists between the inward gravitational force and the outward force due to the gas-pressure gradient. Larger stellar masses cause higher central pressure, resulting in higher core temperature. Hydrogen fusion predominantly occurs through two processes, the proton-proton chain or the CNO cycle. The latter releases energy more efficiently but requires higher core temperatures, and therefore dominates in stars more massive than the Sun. For stars with similar or lower masses than our Sun the fusion will be dominated by the proton-proton chain which has a slower burning rate. This connection between stellar mass and which fusion process dominates means that the stellar mass dictates the time on the main sequence. As M dwarfs have a much lower luminosity than the other main-sequence stars, coupled with that the first branch of the proton-proton chain is the dominating energy source, which has a very slow burning rate, the predicted main-sequence lifetime of these stars is longer than the age of the Universe.

# 2. Exoplanets

Understanding our place in the Universe and if we are alone in this vast space has fascinated human kind throughout its history. Until recently the idea of planets outside the Solar System was only speculative. Everything changed in the mid 1990s with the discovery of a planet orbiting 51 Peg, a solar-like star almost 50 light-years away from us (Mayor & Queloz 1995). Today there are 3672 confirmed exoplanets[1] orbiting a variety of different types of stars. Over the years several techniques have been successfully used in the search for new planets, e.g. the radial velocity method, transit photometry, gravitational microlensing, transit-timing variations and direct imaging. To-date the transit photometry is the most successful technique with 2748 confirmed planets, followed by the radial velocity technique with 728 planets.

## 2.1 Observational techniques

An orbiting planet will cause a very small Doppler shift, see Fig. 2.1, of the spectral lines from the host star that can be detected with a stable, high-resolution spectrograph. The measured semi-amplitude of the radial velocity signal, $K$, depends on several parameters of the planetary system, as given by Cumming et al. (1999):

$$K = \left(\frac{2\pi G}{P}\right)^{1/3} \frac{M_P \sin(i)}{(M_P + M_\star)^{2/3}} \frac{1}{\sqrt{1-e^2}}, \tag{2.1}$$

where $G$ is the constant of gravitation, $P$ the orbital period, $M_P$ the planetary mass, $M_\star$ the stellar mass, $i$ the orbital inclination with respect to the line of sight, and $e$ the orbital eccentricity of the system.

The method was proposed by Struve (1952), however, the discovery of an extrasolar planet took over 40 years because of the very small signals planets give rise to. For example, Jupiter at 5.2 AU from our Sun give a semi-amplitude signal of 12.5 m/s, indicating the required level of instrumental precision. To be able to discover smaller, rocky planets the precision has to be improved with at least an order of magnitude, where Earth give a signal of 0.09 m/s. Today a handful of instruments can achieve sub-meter per second precision, e.g. HARPS at La Silla observatory, HARPS-North at TNG-INAF

[1] Extrasolar Planets Encyclopaedia, updated Oct. 11, 2017

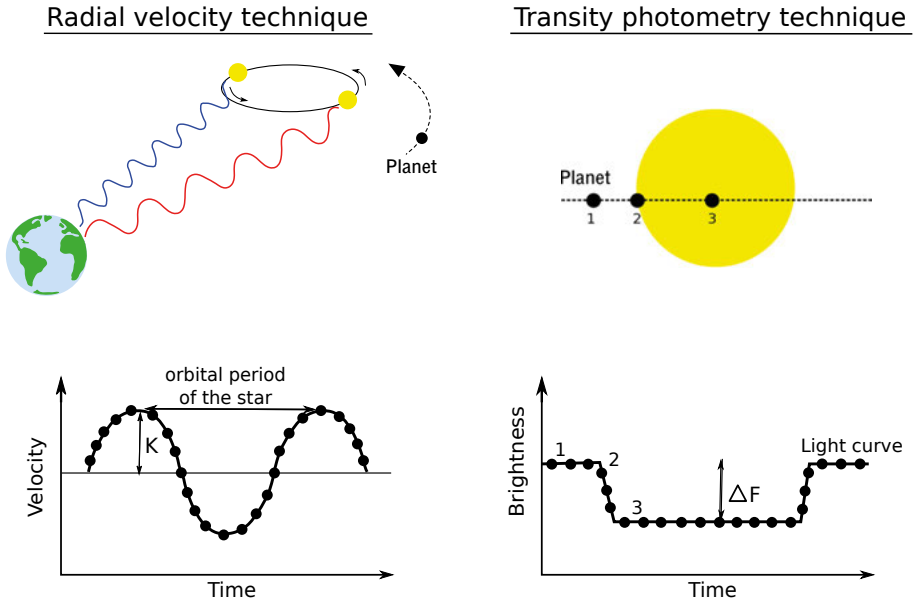


*Figure 2.1.* Schematic picture of the principles behind the radial velocity and transit photometry techniques. The bottom part shows the expected signal from a planet on a circular orbit.

and the HIRES spectrometer at Keck observatory. A promising upcoming instrument is ESPRESSO that will be located at the VLT (Pepe et al. 2014), aiming to give almost an order of magnitude improvement compared to HARPS with a precision of about 0.1 m/s that may be enough to detect Earth-sized planets in the habitable zone around solar-like stars. An alternative way to find Earth-sized planets without the need of increased precision is to change the targets of observation. Because of the signal's dependence on stellar mass ($K \propto M_\star^{-2/3}$), a similarly-sized planet around a smaller star will increase the signal and thereby be easier to detect. This is the idea behind projects like CARMENES at the Calar Alto observatory (Quirrenbach et al. 2014), a dedicated radial velocity survey looking for planets around M dwarfs.

The idea behind the transit photometry technique was proposed by Rosenblatt (1971), but was obstructed by the limitations imposed by Earth's atmosphere. With the successful launch of spacecrafts like CoRoT in 2006 and Kepler in 2009, transit photometry has become the most successful technique for the detection of exoplanets. As a planet transits in the line of sight between us and its host star it occults a small part of the stellar light, causing a slight dip in the observed light curve, see Fig. 2.1. The signal size depends on the ratio between the sizes of host and planet, as outlined in Seager & Mallén-Ornelas (2003) for a planet on a circular orbit:

$$\frac{\Delta F}{F} \propto \left(\frac{R_p}{R_\star}\right)^2. \tag{2.2}$$

As with the radial-velocity technique the signal is very small, and the capabilities of ground-based facilities are severely limited because of Earth's atmosphere giving a detection limit of $(\Delta F/F) \sim 1\%$. This limit the technique to giant planets, as a Jupiter-sized planet around an one solar-mass star cause a drop of the stellar flux of 1.1 x $10^{-2}$. To avoid the atmosphere space-based missions were needed, where a precision of a few times $10^{-4}$ can be achieved, allowing detection of super-Earths, where Earth would result in a drop of 8.4 x $10^{-5}$.

Similarly as for the radial velocity method observations of M dwarfs would increase the signal significantly, for a mid M dwarfs with approximately an orders of magnitude. This advantage enables ground-based facilities to detect super-Earths around M dwarfs, successfully achieved within the MEarth project (Nutzman & Charbonneau 2008) operating from the Fred Lawrence Whipple Observatory in USA and the Cerro Tololo Inter-American Observatory in Chile.

## 2.2 Planet formation

Shortly after 51 Peg b was discovered, a study by Gonzalez (1997) showed that all thus far known planet hosts had enhanced metallicity compared to the Sun. As more exoplanets were discovered a trend of metal enhancement related to the presence of giant planets was confirmed (Santos et al. 2001, 2005; Heiter & Luck 2003; Fischer & Valenti 2005). As the technology improved, especially with the launch of Kepler, a large number of low-mass planets were discovered. In contrast to what was found for stars hosting giant planets, no trend with metallicity was found among hosts of Neptune-size and super-Earth planets (Udry et al. 2006; Sousa et al. 2008, 2011; Adibekyan et al. 2012; Buchhave et al. 2012). An example of the different metallicity distributions for FGK dwarfs hosting low-mass versus giant planets is shown in Fig. 2.2.

To explain the physical mechanism behind the observed planet-metallicity correlation, two different hypotheses were proposed: primordial abundance and self-enrichment. In the scenario of self-enrichment, the observed metal enhancement is a consequence of the planet formation process via engulfment of metal-rich bodies. The capture of these bodies must occur when the star has formed its radiative core and is no longer fully convective, since in a fully convective star the accreted material would not make any significant contribution of the overall metallicity. The self-enrichment scenario would therefore lead to a correlation between metallicity and depth of the convection zone, where the more shallow convective layers are more metal-enhanced (Laughlin & Adams 1997; Pinsonneault et al. 2001). An additional prediction is a difference be-

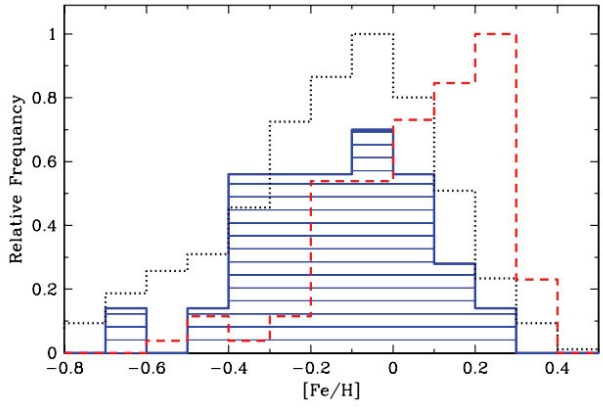


*Figure 2.2.* Metallicity distribution of three different sample of FGK dwarfs. Stars without any detected planets (dotted black), stars with giant planets (dashed red), and stars with only Neptune-size and super-Earth planets (shaded blue).

Image credit: Adibekyan et al. (2012). Reprinted with permission from A&A.

tween the abundance of refractory and volatile elements as the formation of the metal-rich bodies occurs in a rather warm environment, leading to a depletion of volatiles. Detailed chemical studies of large samples of FGK dwarfs with planets have shown that the predicted trend between metal-enhancement and the depth in the convection zone is not present (Fischer & Valenti 2005). Neither was no conclusive evidences for the predicted trend with condensation temperature found (Takeda et al. 2001; Bodaghee et al. 2003; Gonzalez & Laws 2007).

In the other proposed scenario, based on the primordial abundance, the observed metallicity of a star is a trace of the composition of the molecular cloud from which the star and (if any) planets were formed (Pollack et al. 1996). The most widely accepted and tested model for planet formation today is core accretion, which can be traced back as far as the planetesimal hypothesis by Chamberlin (1916). This theory builds on successive agglomeration of material from the proto-planetary disk into larger and larger bodies, from micrometer-sized dust grains to planetesimals, see Fig. 2.3. The correlation with metallicity is believed to arrive from the finite lifetime of the gaseous disk. In order to form a gas giant planet, a planetesimal with a critical mass of around 10 $M_E$ has to form before the gas in the proto-planetary disk disappears, after an estimated time of around 10 Myrs (Haisch et al. 2001; Hillenbrand 2008; Ribas et al. 2014). Simulations have shown that the formation time is highly dependent on the metallicity (Ida & Lin 2004a,b; Kornet et al. 2005; Mordasini et al. 2008), which is expected as the metallicity is a proxy for the amount of solids in the disk.

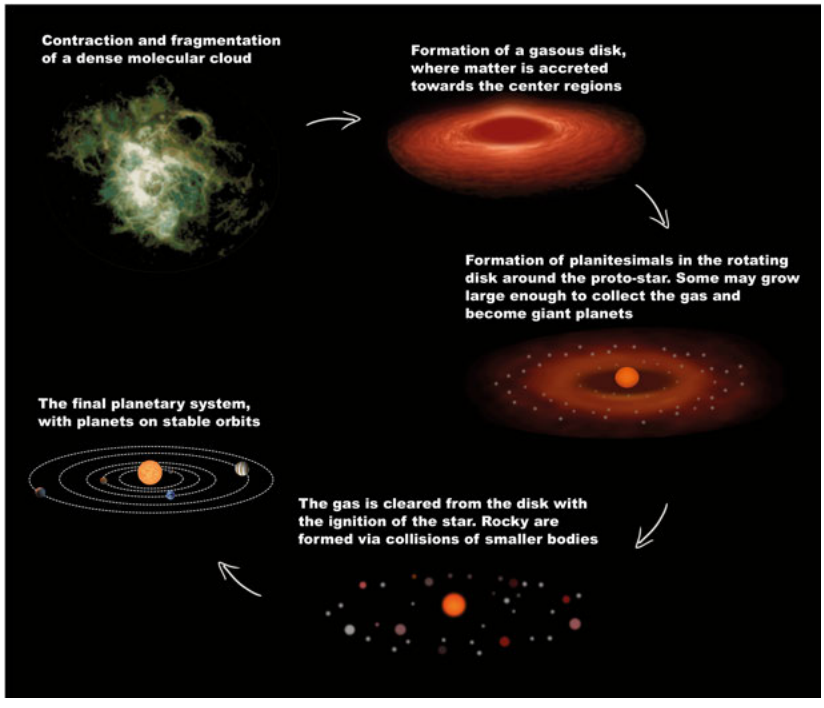


*Figure 2.3.* Planet formation according to core accretion model.

Beyond the trend with metallicity a possible correlation between the occurrence of Jovian planets and stellar mass has been suggested both by observations (Endl et al. 2006; Johnson et al. 2010) and theory (Ida & Lin 2005; Alibert et al. 2011). The stellar mass on the main sequence is linked to the mass of the proto-planetary disk, and a more massive disk would increase the total amount of solids available for planet formation at a given metallicity. The presence of a mass correlation is still debated, and Gaidos & Mann (2014) claim the trend has low statistical significance and a non-correlation cannot be excluded. However, if there indeed exists a mass correlation, this should have consequences for planet formation around low-mass stars. Accurate studies of the chemical composition of M dwarfs with Jovian-mass planets may provide good test cases of the efficiency of planet formation at the low-mass end.

# 3. M dwarfs

M dwarfs belong to a class of stars known as very low-mass (VLM) stars with an approximated mass range of 0.08-0.6 $M_\odot$, comparable to the mass range from early F to late K dwarfs. M dwarfs are, by number, the dominating stellar population making up around 70% of all the stars in the local Galaxy (Covey et al. 2008; Bochanski et al. 2010). Despite this our knowledge of these stars is poor, mainly a consequence of the low temperature that gives rise to complex molecule-dominated spectra.

## 3.1 A spectroscopic challange

The low effective temperature of M dwarfs of approximately 2700 to 4000 K has three main effects on the stellar atmosphere: (1) Formation of molecular species, which all have a rich spectrum due to the many rotational and vibrational bands. (2) Hydrogen mainly exists in the form of $H_2$ and H, rather than $H^-$ and H as in FGK dwarfs, and (3) a reduced degree of ionization.

Accurate spectral analysis requires good knowledge of the continuum opacity. For FGK dwarfs $H^-$ is the most important opacity source, but for M dwarfs, especially toward the later spectral types, molecules are becoming an increasingly important opacity source. This is problematic as the data for most molecules is often insufficient (Allard et al. 2013). In addition to the continuum problem the rich rotational and vibrational spectra leave almost no atomic lines unblended (see Fig. 3.1).

Dominating species are TiO and $H_2O$, but also other oxides and hydrides are important, e.g. VO, CO, CaH, MgH, CaOH, FeH, CrH. In the wavelength region between 4000 and 9500 Å TiO features start to be visible in mid-K dwarfs with increasing influence with decreasing effective temperature until spectral type M6. For later spectral types VO takes over as the dominating molecule in this wavelength region. The increased opacity in the visual caused by the TiO and VO bands shifts much of the flux into the near-infrared. Hence, M dwarfs are much brighter in the infrared than in the optical and despite their numbers none of them are visible to the naked eye. At wavelengths beyond 13500 Å water is the dominating molecule, while some strong CO bands are present between 23000 and 24000 Å. At intermediate wavelengths between the TiO and $H_2O$ dominated regions, from 11000 to 13500 Å, the spectra are much less affected by molecular lines. For spectral types earlier than M5 this wavelength region mainly contains atomic lines and weak FeH lines. In colder stars water bands, but also the FeH lines, are becoming increasingly stronger.

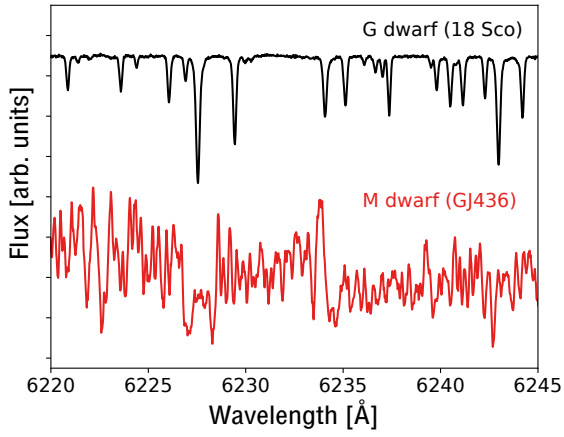


*Figure 3.1.* Short wavelength interval from observed spectra from a G dwarf (black) and a M dwarf (red). The spectra were obtained with the high-resolution UVES spectograph within the Gaia-ESO survey.

## 3.2 M dwarfs as planet hosts

In the early days of exoplanet research M dwarfs were largely excluded, something that has started to change in the last decade because of the technical advantages they provide. Their smaller mass and radius increase the observable signal of the two most used detection techniques, as described in Sect. 2.1. Because of their lower luminosity the habitable zone lies closer to M dwarfs, giving planets in the habitable zone shorter orbital periods than the year-long orbit around G dwarfs like the Sun. This allows multiple observations per year, essential for transit spectroscopy. The efficiency of observations is especially important for space missions like the upcoming James Webb Space Telescope (JWST) with a limited operational lifetime. Several studies also predict a higher occurrence rate of planets in the mass range of 1–4 $M_E$ around M dwarfs compared to FGK dwarfs (Dressing & Charbonneau 2013, 2015; Mulders et al. 2015). Coupled with the fact that they are the dominating type of stars, we can expect that the majority of all small planets are orbiting M dwarfs.

Even if the possibility to detect Earth-sized planets in the habitable zone of an M dwarf is larger than for solar-like stars, the conditions for life on these planets are vastly different. M dwarfs are known to be very magnetically active (Johns-Krull & Valenti 1996; West et al. 2004; Shulyak et al. 2010), and to have a large spot coverage and flaring events. This exposes the planets to high levels of X-ray and UV emission. The small orbital distance to the host star means that most of them will be tidally locked, with the risk to evaporate away much of the atmosphere or ocean on the illuminated side if the atmosphere is not thick enough to be able to redistribute the heat.

# 4. Spectroscopy

The stellar atmosphere is the transition area where material becomes optically thin that energy in the form of the photons, originating in the nuclear processes deep within the stellar core can escape and may be observed by us. The stellar atmosphere consists of several layers, e.g. photosphere, chromosphere and corona, where different layers are governed by widely different physical conditions. In this thesis the focus will be on the photosphere since a major part of the visual and near-infrared spectra is formed within this layer. In order to understand a stellar spectrum we need a theoretical description of all processes of importance affecting the photons on their path from the stellar interior until they escape. Deep inside a star the pressure and density is high. The short mean free path, together with frequent collisions, means that the radiation field is efficiently coupled to the gas and is well described by the Planck function. Closer to the surface the mean free path increases and some of the stellar light escapes the atmosphere, resulting in a non-local and non-isotropic radiation field. However, even though strict thermodynamic equilibrium is no longer valid a common assumption in spectroscopy is local thermodynamical equilibrium (LTE). This means that thin photospheric layers are thermodynamically and radiatively characterized by the local gas temperature. In this chapter we assume LTE, an assumption discussed briefly in Sect. 4.4.

## 4.1 Stellar model atmospheres

A stellar model atmosphere should describe all of the physical conditions that affect the formation of the stellar spectrum. Several codes exist today: MARCS (Gustafsson et al. 2008), ATLAS (Castelli & Kurucz 2004), and PHOENIX (Hauschildt & Baron 1999), to mention some of the most commonly used. The majority use the following assumptions to simplify calculations: 1) Plane-parallel geometry, such that all physical variables depend only on the depth. 2) Local thermodynamic equilibrium, as described above. 3) All structures on the surface, such as star spots and granulation patterns, are assumed to have limited influence. 4) The effects of magnetic fields are negligible.

In gas where collisions, rather than radiation, dominate the excitation of atoms the assumption of LTE is valid. Under this assumption the population of a given ionization stage for any element at temperature $T$ can be described by a combination of the Boltzmann and Saha equations. The Boltzmann equation

is used to calculate the number of atoms per unit volume in a given energy level as a fraction of all atoms of that species:

$$\frac{n_j}{N} = \frac{g_j}{Z} e^{-\chi_j/kT} \tag{4.1}$$

where $N$ is the total number of atoms in the ionization stage, $n_j$, $g_j$ and $\chi_j$ are the number density, statistical weight and excitation energy of level $j$, and $k$ is the Boltzmann constant. $Z$ is the partition function, which is defined as:

$$Z = g_0 + \sum g_j e^{-\chi_j/kT} \tag{4.2}$$

where $g_0$ is the statistical weight of the ground state.

The Saha equation is used to calculate the ratio of the number of particles in two subsequent ionization stages with ionization potential $\chi_i$ in a collision-dominated gas, assuming that the electron pressure ($P_e$ in cgs units) can be calculated by the ideal gas law:

$$\frac{N_{i+1}}{N_i} = \frac{1}{P_e} 0.667 \frac{Z_{i+1}}{Z_i} T^{5/2} e^{-\chi_i/kT} \tag{4.3}$$

## 4.2 Spectrum synthesis

Modeling the shapes and strengths of atomic lines can provide us with a lot of information about a star. The properties of the spectral lines arise from the interplay between the line absorption and all physical parameters in the plasma such as temperature, pressure, radiation field, velocity field and magnetic field. Due to computational limitations no code is yet able to include all physical processes in full detail, and depending on the object of interest different simplifications are made.

In order to calculate a synthetic intensity spectrum we need to known how the propagation of radiation through a medium is affected by absorption, emission, and scattering processes. This is done by solving the radiative transfer equation (RTE), describing the intensity $I$ along a ray at frequency $\nu$. The differential form of the RTE is

$$\frac{dI_\nu}{d\tau_\nu} = -I_\nu + S_\nu, \tag{4.4}$$

where $\tau_\nu$ is the optical depth and $S_\nu$ is the source function. By computing

and integrating the emerging intensity at wavelengths over the whole stellar surface we can compute the spectrum, which can be compared to our observed spectrum.

The source function depends on the line emission and absorption coefficients $j_\nu^l$ and $l_\nu$, and the continuum emission and absorption coefficients $j_\nu^c$ and $\kappa_\nu$. Defining the line source function as $S_l = j_\nu^l / l_\nu$ and continuum source function as $S_c = j_\nu^c / \kappa_\nu$, we can write the total source function as:

$$S_\nu = \frac{S_l + (\kappa_\nu / l_\nu) S_c}{1 + \kappa_\nu / l_\nu} \tag{4.5}$$

The line source function depends on the level population, which in turn depends on the transition probabilities for all absorption and emission processes. These probabilities are given by the Einstein coefficients; $A_{ul}$: Spontaneous de-excitation, $B_{ul}$: Stimulated de-excitation caused by a passing photon, and $B_{lu}$: Radiative excitation by absorption of a photon. In addition the possibility of collisional interactions exists where atoms collide causing thermal excitation or de-excitation, given by the probability constants $C_{lu}$ and $C_{ul}$. Only including radiative processes yields the following line source function:

$$S_l = j_\nu^l / l_\nu = \frac{n_u A_{ul} \Psi(\nu)}{n_l B_{lu} \Phi(\nu) - n_u B_{ul} \Phi(\nu)}, \tag{4.6}$$

where $\Psi(\nu)$ and $\Phi(\nu)$ specify the frequency dependence of emission and absorption. Assuming LTE simplifies this expression, where $\Psi(\nu) = \Phi(\nu)$, the level populations are given by the Boltzmann distribution, and $S_l$ is given by the Planck function.

## 4.3 The strength of absorption lines

The number of absorbers of a given element is calculated along a path, meaning that with increased continuum opacity the optical path will become shorter and the emerging flux in the line will come from higher up in the atmosphere. This is of importance due to the temperature gradient that exists in the photosphere, with increasing temperature towards the bottom. In a region where the continuum opacity is low we can see deeper in the photosphere where the temperature is higher, with a higher emerging flux. On the contrary, in the region of lines, especially in line cores, the opacity is high and the majority of the photons are from layers higher up in the atmosphere, i.e. layers with cooler temperatures, causing the formation of an absorption spectrum. This also means that both the line opacity and continuum opacities are of importance for the line strength. For weak lines the line strength is proportional to the line opacity and inversely proportional to the continuum opacity,

$R = l_\nu / \kappa_\nu$. For solar-like stars $\kappa_\nu$ is mainly determined by the opacity from $H^-$, while for M dwarfs molecular line opacities are of equal importance.

The strength of an absorption line depends directly on the absorption coefficient ($l_\nu$), which in turn depends on the number of absorbers, in LTE given by the Boltzmann and Saha equations. From this we can see that the line strength depends on the temperature, electron pressure and the atomic constants ($Z$, $\chi$, and $g$). For the temperature dependence four cases have be identified (Gray 2005, p. 317), where the first is most important for M dwarfs: weak lines of neutral species with the element mostly neutral. In this case $R = \text{constant}\ \frac{T^{5/2}}{P_e} e^{-(\chi+0.75)/kT}$ (assuming that $\kappa_\nu$ is dominated by $H^-$ bound-free absorption). Weak lines are therefore sensitive to the temperature, but in order to do a good determination we need several lines of different excitation energies. The pressure mainly affects three types of spectral lines: ionized lines, the wings of strong lines, and hydrogen lines in hot stars through the linear Stark broadening. This causes a limitation for M dwarfs since none of these type of lines are very abundant due to their low effective temperature.

Finally, the number of absorbers of a given element will influence the spectral line strength and shape through what is known as the curve of growth. For weak lines an increase of absorbers, i.e. increase of element abundance, will linearly increase the line strength. At some point the line becomes saturated where the flux in the core can not decrease any further, starting the formation of line wings. The last stage occurs if the opacity depth in the wings become significant compared to the continuum opacity.

## 4.4 The assumption of LTE in M dwarfs

Under certain conditions the assumption of LTE is no longer valid, where the two most likely scenarios for M dwarfs is insufficient number of collisions to counteract radiative transitions that lead to non-equilibrium level populations, and the influence from non-local phenomena, for example radiation from the chromosphere. In solar-like stars collisions with electrons provide an efficient restoring mechanism toward LTE. For M dwarfs the situation is different because of the much lower electron temperature and electron density. As collisions with $H_2$ or He are not as efficient, Hauschildt et al. (1997) argued that this may result in non-equilibrium level populations.

The vast majority of the work on non-LTE effects has been conducted for FGK dwarfs and giants, as deviations from LTE in general increase with higher effective temperature, lower surface gravity and towards very metal-poor stars (Asplund 2005). This indicates that the effects for M dwarfs should be limited, but to our knowledge no detailed study of non-LTE effects exists for M dwarfs.

# 5. Metallicity

In the creation on the Universe only three elements were created: hydrogen, helium, and tiny amounts of lithium. All heavier elements have been created later by a broad variety of processes in different astronomical sites; fusion of lighter elements in the stellar core, the *r*-, *s*- and *p*-processes in asymptotic giant branch stars, novae, supernovae and kilonovae, and via spallation in the interstellar medium. This leads to a continuous enrichment, where each generation of stars is slightly enriched in metals compared to the previous one. In this work we use the following definition of metallicity:

$$[\mathrm{M/H}] = \log\left(\frac{N_M}{N_H}\right)_\star - \log\left(\frac{N_M}{N_H}\right)_\odot , \tag{5.1}$$

where $N_H$ is the number of hydrogen atoms and $N_M$ the number of all atoms heavier than hydrogen and helium.

For solar-like stars the metallicity, and abundances of individual elements, can be determined with a good level of accuracy from the analysis of atomic lines. This can either be done via the measurement of equivalent widths or by fitting synthetic spectra to the line shapes and depths. The huge number of molecular lines in the spectra of M dwarfs leave almost no unblended atomic lines and cause a pseudo-continuum as described in Sect. 3.1. This severely limits the usefulness of both of these methods for M dwarfs working with spectra in the optical. Therefore many previous studies have relied on empirical calibrations using photometric data or spectral indices.

## 5.1 Photometric calibrations

Photometric calibrations build on the fact that the star's metallicity is linked to its magnitude and color, where previous calibrations used the absolute $K_\mathrm{S}$ magnitude and the $V - K_\mathrm{S}$ color. For a star of a given mass, the higher metal content result in a lower effective temperature and thereby a lower bolometric luminosity. The increased metallicity also makes the molecular bands, mainly the TiO bands, in the visual stronger and the increased opacity shifts flux into the near-infrared. In the visual these two effects will enhance each other, making these magnitudes very sensitive to the stellar metallicity, while in the infrared the effects counteract each other. The effect on stellar spectra of varying metallicity at a fixed mass is shown in Fig. 5.1, showing calculated

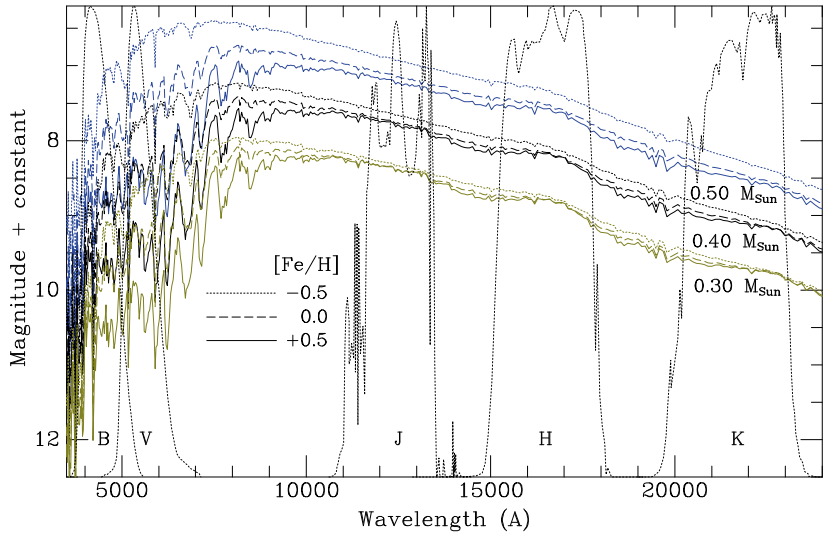


*Figure 5.1.* Binned fluxes in magnitude units from MARCS models with three masses and for each mass three different metallicities ([Fe/H] = −0.5, 0.0, and +0.5). The atmospheric parameters correspond to 5 Gyr Dartmouth isochrones (G. Feiden, priv. comm.). The photometric passband transmission curves are shown on a linear scale. Figure courtesy B. Edvardsson.

spectra using a plane-parallel MARCS models. The strong metallicity sensitivity of the TiO molecular bands in the $B$ and $V$ bands is clearly visible. For a 0.4 solar mass model the difference in the absolute $V$ magnitude is around 1.6 mag between −0.5 and +0.5 dex, while the absolute $K_S$ magnitude only changes by 0.13 mag.

The use of photometric data for empirical calibrations of M dwarfs was pioneered by Bonfils et al. (2005), inspired by the dispersion in the mass-luminosity relation for the $V$ magnitude found by Delfosse et al. (2000). Using a sample of M+FGK binaries, they found that the metallicity could be described by a second degree polynomial function of the absolute $K_S$ magnitude and $V - K_S$ color. A couple of years later Johnson & Apps (2009) investigate the reason behind the lower mean metallicity Bonfils et al. (2005) found for a volume-limited sample of M dwarfs compared to a sample of FGK dwarfs. They concluded this mainly was due to lack of metal-rich stars in the used calibration sample, and used six M dwarfs in binaries with super-solar metallicity together with two volume-limited samples of M and K dwarfs to determination of a new calibration. Furthermore, they argue that the volume-limited samples of M dwarfs and FGK dwarfs should have the same mean metallicity. Schlaufman & Laughlin (2010) on the contrary argued that the enforcement of the mean metallicity was incorrect because the different type of stars not nec-

essary belong to the same kinematic populations. To ensure this they used data from the Geneva-Copenhagen Survey (Nordström et al. 2004; Holmberg et al. 2009). Using stellar evolution models by Baraffe et al. (1998) they argued that the metallicity would cause a shift in color, rather than in magnitude as used by Johnson & Apps (2009). The derived photometric relation by Schlaufman & Laughlin (2010) was later refined by Neves et al. (2012) slightly using a larger calibration sample.

## 5.2 Spectroscopic calibrations

As many M dwarfs still lack parallax measurements, it limit the use of photometric calibrations since most make use of the absolute magnitude. Empirical calibrations based on spectral features have provided a way forward. Even though Woolf et al. (2009) provided a method to use spectral indices of TiO and CaH in the visual, the success came with the use of low- or moderate resolution spectra in the infrared $J, H$ and $K_S$ bands. As these wavelength regions are less affected by molecules some atomic lines, mainly from alkaline or alkaline Earth metals, are visible even in low resolution spectra. This approach was pioneered by Rojas-Ayala et al. (2010), continued in Rojas-Ayala et al. (2012). The calibration was determined using the equivalent widths the Na I doublet (2206 and 2209 nm) and Ca I triplet (2261, 2263, and 2265 nm). As for photometric calibrations external calibration is needed, provided by several M dwarfs in binaries. The effect of the effective temperature on the molecule-dominated spectra was accounted for using a spectral index calibrated against synthetic spectra of PHOENIX models (Allard & Freytag 2010). Spectroscopic empirical relations using metallicity sensitive lines in different infrared bands have since been expanded by Terrien et al. (2012), Mann et al. (2013), Newton et al. (2014), and Mann et al. (2014), among others.

## 5.3 High-resolution spectral analysis

Despite the spectroscopic challenges presented by the molecule-dominated optical spectra of M dwarfs described in Sect. 3.1 there have been a few attempts to use atomic lines in high-resolution optical spectra to determine the metallicity (Valenti et al. 1998; Woolf & Wallerstein 2005; Bean et al. 2006b). The accuracy and applicability of this method is currently questionable due to the lack of complete molecular line lists. This may however change in the future with projects like the ExoMol database (Tennyson et al. 2016), which aim to provide extensive line lists for most relevant molecules.

The introduction of high-resolution spectrographs operating in the infrared provided a new window for the investigation of M dwarfs. Within this wavelength region the continuum level and individual atomic lines can be identified

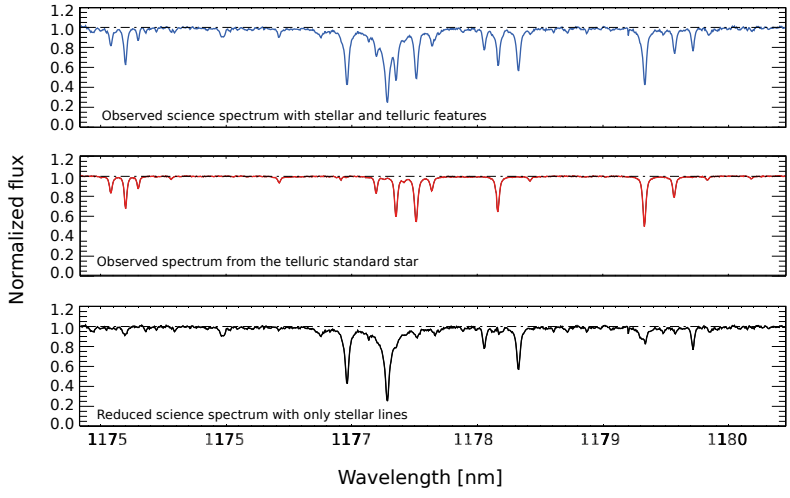


*Figure 5.2.* An example of a continuum rectified and wavelength corrected spectrum in a short wavelength interval for GJ 179, spectral type M2V. The top panel shows the science spectrum, the middle panel the spectrum from the telluric standard star and the bottom panel the science spectrum where the telluric lines have been removed. The horizontal pot-dashed line at 1.0 is for visualization of continuum regions. The figure is taken from Paper II.

(cf. Sect. 3.1). Figure 5.2 shows an example of an M dwarf observed with the CRIRES spectrograph at a resolution of 50 000. As the high-resolution infrared spectra allow for continuum rectification and identification of individual atomic lines, the metallicity can be determined using similar methods as for solar-like stars by fitting the observed line profiles with synthetic spectra or calculations of the equivalent widths. The achievable accuracy of the spectral analysis will depend on several things: the quality of the observed spectra, the assumptions made in the model atmosphere, the accuracy and completeness of atomic and molecular line data, that the radiative transfer code incorporates all relevant physics, that there is a sufficient number of lines that are sensitive to different stellar parameters, and so on.

# 6. Metallicity determination using high-resolution infrared spectra

The use of infrared spectra obtained with high-resolution facilities to determine the metallicity of M dwarfs was pioneered by Önehag et al. (2012), a method possible by the limited amount of molecular lines in the J band allowing individual stellar lines to be identified. The first two papers included in this thesis discuss a continued application of this method. We analyzed several M dwarfs with different spectral types in binaries with warmer solar-like stars to test the reliability of the approach and compared the results from the high-resolution studies with available empirical calibrations. We summarize the main results in this section, while more details can be found in Paper I (Lindgren et al. 2016) and Paper II (Lindgren & Heiter 2017).

## 6.1 Target selection and observations

To be able to check the reliability of metallicity determination using the fit of synthetic spectra to atomic lines in high-resolution infrared spectra the first set of observations included several M+FGK binaries. In addition a number of individual M dwarfs, mainly known planet hosts, were included. This selection gave a rather limited range in effective temperature and metallicity. In the second set of observations stars within a wider range of spectral type were included and furthermore, by using the photometric calibration by Schlaufman & Laughlin (2010), we aimed to include mainly stars with solar and sub-solar metallicity.

Observations were conducted at the Very Large Telescope (VLT, European Southern Observatory) that consists of four 8.2 m Unit Telescopes (UT1 to UT4, a.k.a. Antu, Kueyen, Melipal and Yepun) and four movable 1.8 m Auxiliary Telescopes. VLT is located at Paranal Observatory, at 2635 m altitude in the Atacama desert in northern Chile. The observations were carried out with the high-resolution instrument CRIRES (CRyogenic high-resolution InfraRed Echelle Spectrograph, Kaeufl et al. 2004), mounted at UT1 from 2006 to 2014. All stars were observed at a handful of wavelength settings in the *J* band (1100–1400 nm) with a slit width of $0\farcs4$ resulting in resolving power of around 50 000.

## 6.2 Spectral analysis

The spectral analysis was done with the software package Spectroscopic Made Easy (SME, Valenti & Piskunov 1996; Piskunov & Valenti 2017). The synthetic spectra were calculated by solving the integral form of the radiative transfer equation, using an adaptive wavelength grid to achieve uniform precision. We used the stellar atmosphere models from the MARCS grid (Gustafsson et al. 2008), more precisely a subset of the MARCS-2012 models for cool dwarfs, which covers effective temperatures down to 2500 K and surface gravities up to 5.5 log(cm $s^{-2}$).

Because of the properties of the CRIRES spectrograph, at the time of our observations, where two of four detector chips were heavily vignetted and contaminated by overlapping orders, the final reduced spectra only had around 60 Å of usable data for each star. This gave 15–20 usable atomic lines from the species Ca, Fe, Ti, Mg, Si, Cr, Co, and Mn. As a consequence of the limited wavelength coverage of the observations there was not enough diversity in the line parameters to make the spectra sensitive to all stellar parameters. Therefore the effective temperature and surface gravity were determined prior to the metallicity, mainly using different photometric calibrations; $\log g$: Delfosse et al. (2000); Bean et al. (2006a); Mann et al. (2015); Benedict et al. (2016), $T_{\rm eff}$: Casagrande et al. (2008); Mann et al. (2015).

### 6.2.1 Effective temperature using FeH lines

An alternative method to determine the effective temperature for M dwarfs was explored, using the strength of the FeH lines present in the observed spectra in the *J* band. As the abundance of molecular species tightly depends on the temperature in the atmosphere a degeneracy is expected between the effective temperature and metallicity. The degree of degeneracy was explored by calculating a grid of 2583 synthetic spectra with SME with varying $T_{\rm eff}$ and [M/H]. The best-fit stellar parameters were found by calculations of the $\chi^2$ values compared to the observations of around 50 lines of the FeH molecule. We found that the minimum $\chi^2$ value for M dwarfs with $T_{\rm eff}$ 3200–3500 K only depends on the effective temperature. For warmer M dwarfs the lowest $\chi^2$ at a given metallicity is found at slightly different temperatures. This is shown in Fig. 6.1; to the left an example of a cold M dwarf showing negligible degeneracy and to the right a warmer star where $\chi^2$ depend on both the effective temperature and metallicity. For M dwarfs warmer than 3800 K the FeH lines become too weak and blend in with the continuum. When comparing the results for M dwarfs with none or little degeneracy (3200–3500 K), the determined effective temperatures agree within $\pm$150 K with other spectroscopic methods for M dwarfs (Rojas-Ayala et al. 2012; Lépine et al. 2013; Mann et al. 2015).

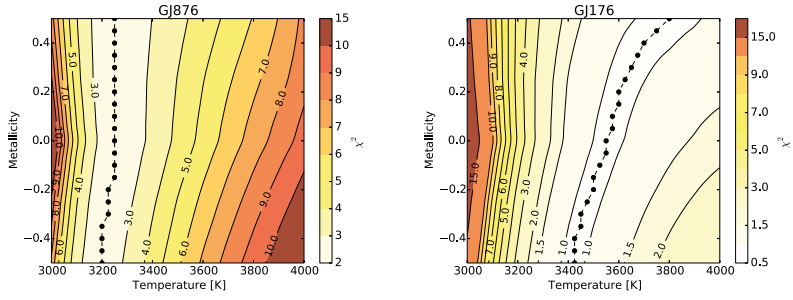


*Figure 6.1.* Demonstration of the fit to the FeH lines present in the *J* band with a grid of synthetic spectra with varying effective temperature and metallicity. The contour plots show the calculated $\chi^2$ for each combination, where the dotted lines indicate the temperature with the best fit for each step in metallicity. The figures are taken from Paper I.

### 6.2.2 Validation of the metallicity determination

The results for both components in the observed M+FGK binaries were used to ensure that the method to determine the metallicity of M dwarfs is reliable, given the constraints posed by the limited wavelength range of our observations. The values derived for the components lie within 0.05 dex, where the M dwarfs span a large range in effective temperature from 3200 K to 3900 K. The results compare well with optical high-resolution studies of the warmer components (Valenti & Fischer 2005; Santos et al. 2005; Takeda et al. 2005; Luck & Heiter 2006; Gonzalez et al. 2010), and with a calculated mean of previous optical studies published after the year 2000, see Table 6.1.

### 6.2.3 Comparison with empirical calibrations

The combined sample from Paper I and Paper II contains 24 stars (excluding a handful of stars with lacking or unreliable photometry). The sample has a range of $T_{\rm eff} \simeq 3200$ to 4500 K and [M/H] $\simeq -0.5$ to +0.4 dex. This range is sufficient to compare the performance of different spectroscopic calibrations (Rojas-Ayala et al. 2012; Terrien et al. 2012; Newton et al. 2014; Mann et al. 2013, 2014, 2015) and photometric calibrations (Bonfils et al. 2005; Johnson & Apps 2009; Schlaufman & Laughlin 2010; Neves et al. 2012). No comparison could be done with Terrien et al. (2012) and Newton et al. (2014) because of too few stars in common.

Figure 6.2 show the calculated differences in metallicity between the values we obtain with high-resolution spectroscopy compared to those given by different empirical calibrations. A good agreement was found compared to the results by Rojas-Ayala et al. (2012) and Mann et al. (2015), shown in sub-figure 6.2(b) and 6.2(c). The average differences compared to our high-

**Table 6.1.** *Comparison of determined metallicity between binary components and with the average literature value.*

| Target | Metallicity [dex] | $T_{\rm eff}$ [K] | Ref. metallicity |
|---|---|---|---|
| HIP12048 A | $+0.13 \pm 0.04$ | $5802 \pm 43$ | +0.14 (0.04) |
| HIP12048 B | $+0.14 \pm 0.15$ | $3225 \pm 100$ | |
| GJ527 A | $+0.22 \pm 0.04$ | $6446 \pm 90$ | +0.28 (0.07) |
| GJ527 B | $+0.21 \pm 0.10$ | $3325 \pm 100$ | |
| GJ250 A | $-0.03 \pm 0.07$ | $4676 \pm 150$ | −0.04 (0.10) |
| GJ250 B | $-0.07 \pm 0.04$ | $3550 \pm 100$ | |
| HIP57172 A | $+0.15 \pm 0.06$ | $5030 \pm 51$ | +0.17 (0.05) |
| HIP57172 B | $+0.16 \pm 0.13$ | $3900 \pm 100$ | |

**Note:** The reference metallicity is the average value from the literature for the warmer component. The standard deviation is given in parentheses.

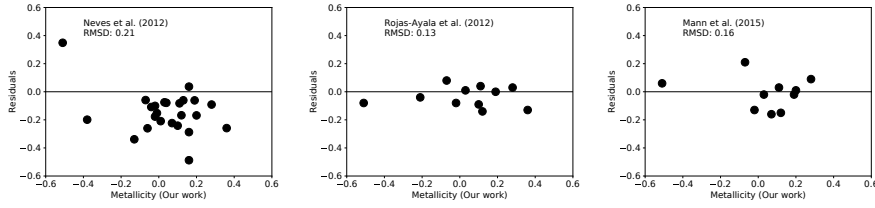


*Figure 6.2.* Calculated residuals between the metallicity of 24 stars; comparing our high-resolution results with the three empirical calibrations (left to right) by Neves et al. (2012), Rojas-Ayala et al. (2012) and Mann et al. (2015).

resolution results are less than 0.05 dex with root-mean-squared deviations of around 0.15 dex. The comparison with the different photometric calibrations is less satisfying. An example for Neves et al. (2012) is shown in Fig. 6.2(a). The remaining photometric calibrations give similar results, where large differences are found for individual stars and the calculated root-mean-squared deviations lie between 0.2 and 0.3 dex. The majority of the calibrations furthermore give a lower mean metallicity than the high-resolution analysis.

# 7. Determination of a new photometric calibration

The intrinsic faintness of M dwarfs, in combination with the complexity of their spectra, makes the acquisition and analysis of high-resolution spectra time-consuming. In practice, for studies of large samples of hundreds or thousands of M dwarfs empirical calibrations are more suitable. Realizing that many of the available photometric calibrations show a low precision coupled with systematic differences compared to the results from our spectroscopic high-resolution study we decided to use our sample of M dwarfs from Paper I and Paper II to determine a new calibration. We summarize the main results in this chapter, while more details can be found in Paper III (Lindgren et al., 2017, to be submitted).

## 7.1 Calibration sample

The number of stars from Paper I and Paper II with metallicities below $-0.1$ dex was not sufficient to give a reliable calibration at low metallicity. To expand the calibration sample several M dwarfs in binaries with FGK dwarfs were included; nine with sub-solar metallicity and one super-solar, see Fig. 7.1. For these 10 M dwarfs the metallicity was taken from the literature determined by high-resolution spectral analysis of the warmer component. The combined sample covers a range in metallicity from around $-0.6$ to +0.4 dex and spectral types from M4.5 to K5 ($T_{\rm eff} \simeq$ 3150–4550 K), with a gap in temperature between the star with the highest effective temperature and the remaining sample.

## 7.2 A refined photometric calibration

As described in Sect. 5.1 metallicity affects the stellar color and magnitude, where a metal-rich M dwarf will have a redder (visual−infrared) color than a metal-poor star. Similar to previous works we assumed that the metallicity can be described as a polynomial function of color and absolute magnitude, where the coefficients of the polynomial were determined through a weighted least-squares solution against the calibration sample. All previous calibrations used functions without mixed terms, an assumption we tested with two statistical

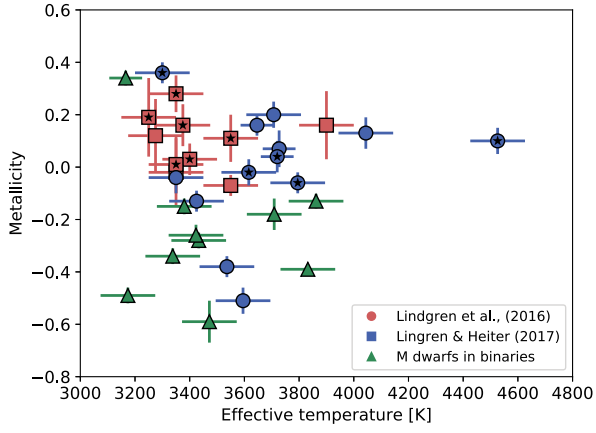


*Figure 7.1.* Distribution in the metallicity - effective temperature plane of the stars in the calibration sample. Metallicities are taken from three difference sources, marked with different symbols. Symbols with a little black star indicate that it is a confirmed planet host.

tests[1,2] evaluating the performance of six polynomials of increasing degree and with and without a mixed term of the color and magnitude. We found that the inclusion of a cross-term was important, and that the following polynomial form was clearly favorable compared to the other relations:

$$[\mathrm{M/H}] = a_0 + a_1 C + a_2 M + a_3 CM, \tag{7.1}$$

where $C$ is the color and $M$ is the absolute magnitude.

Previous photometric calibrations have only used the $V - K_S$ color, but we found that the $V - (JH)$ and $B - (JHK_S)$ colors gave statistically comparable results. Figure 7.2 shows a graphic representation of the new photometric calibration using the $V - K_S$ and $B - K_S$ colors, compared to theoretical iso-metallicity curves at [Fe/H] = $-0.5$, 0.0, and $+0.5$ dex (see Paper III for details on the theoretical data). A reasonably good agreement in both shape and slope was found between the observational and theoretical curves.

Our calibration shows substantially improved statistical characteristics compared to the calibrations by Bonfils et al. (2005), Johnson & Apps (2009), Schlaufman & Laughlin (2010), and Neves et al. (2012). Furthermore, the metallicities calculated from Eq. 7.1 compare well with the metallicities determined from the spectroscopic calibrations by Rojas-Ayala et al. (2012) and Mann et al. (2015). Without applying any restrictions on the uncertainty of

[1] 5-fold cross-validation (Breiman & Spector 1989)
[2] Corrected Akaike information criterion (Burnham & Anderson 2004)

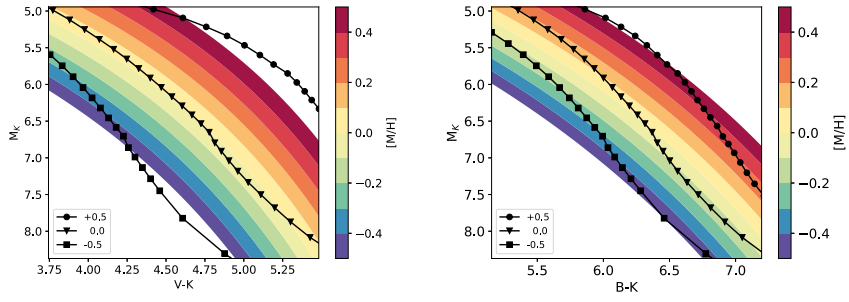


*Figure 7.2.* Graphic representation of our photometric relations. The over-plotted black symbols connected with lines are synthetic iso-metallicity lines at metallicities [M/H] = −0.5, 0.0, and +0.5, calculated using MARCS models and 5 Gyr Dartmouth isochrones. The synthetic iso-metallicity lines were shifted by +0.4 mag in color to match the observed ones at 3500 K. The figure is taken from Paper III.

the photometry or parallax the calculated root-mean-square-deviation is only about 0.05 dex higher than the uncertainties given for the two spectroscopic calibrations.

## 7.3 Metallicity distribution of M dwarf planet hosts

The improved photometric calibration together with the discoveries of new exoplanets around M dwarfs in the past few years allows us to explore how the metallicity distribution among M dwarf hosts compares with the finding for FGK dwarfs discussed in Sect. 2.2. Figuse 7.3 shows the different metallicity distributions of M dwarfs with two types of planets; low-mass ($<$0.05 $M_J$) and giant planets ($>$0.3 $M_J$). For comparison a volume-limited sample from the MINMS survey (Ward-Duong et al. 2015) was included. The similarities with the distributions for FGK dwarfs as shown in Fig. 2.2 provide an indication for a giant planet – metallicity correlation present also among M dwarf hosts, even though the analysis is currently limited by low number statistics.

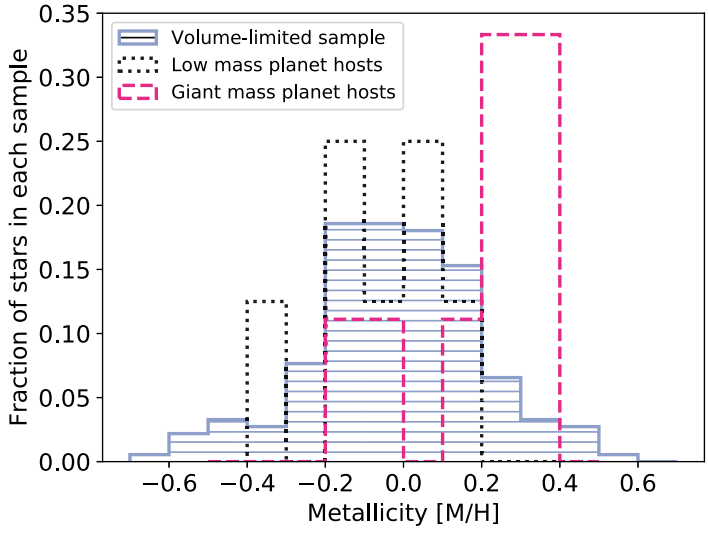


*Figure 7.3.* Metallicity distribution of three samples; a volume-limited sample of stars with spectral types K7-M6, M dwarfs with confirmed low-mass planets, and M dwarfs hosting at least one Jupiter- or Saturn-mass planet. The figure is taken from Paper III.

# 8. Conclusions and Outlook

M dwarfs constitute about 70% of all stars in the local Galaxy, but in order for the community to be able to include these stars in their research a certain accuracy of the determined stellar parameters is needed. This has historically been difficult because of the molecular dominated spectra. Partly driven by the interest from the exoplanet community, great effort has been done in the last couple of decades to understand the processes that govern these cold, small and complex stars. In this thesis I have shown that a careful analysis of high-resolution spectra obtained in the *J* band can provide reliable metallicities for M dwarfs with effective temperatures down to approximately 3100–3200 K. Beyond this point the spectra are affected by a large amount of water lines, and further investigations of how reliable this approach is for these even colder stars are needed. For slowly rotating stars with spectral types M4 to K7 we find uncertainties of 0.05–0.1 dex, provided that the observations have a S/N ratio above 100.

In the second part of the thesis I showed that we could use this sample of M dwarfs to determine an improved empirical photometric calibration. The new relation shows improvements in statistical properties compared to previous calibrations. While previous calibrations have been limited to the $V - K$ color we showed that other combinations of visual and infrared magnitudes give similar results. Applying the determined calibration to a sample of M dwarfs with and without giant planets we could show a plausible metallicity correlation, similar to that of FGK dwarfs. The similar metallicity distribution may be an indication that the formation of Jupiter-sized planets in the proto-planetary disks of M dwarfs do not require a stronger metal enhancement than their FGK counterparts despite the lower disk mass. It is however important to remember that this type of studies for M dwarfs still contains relatively few stars, and no strong conclusions can be made. The situation should improve soon with the parallaxes provided by the Gaia mission so that the M dwarf hosts discovered by the Kepler mission can be included.

To continue the work presented in this thesis there are two things that could be explored in the near future. First is the expansion to spectral types later than M4, the coldest star analyzed in the papers included in this thesis. For M dwarfs with effective temperatures below 3100 K even the *J* band starts to be strongly affected by molecular lines, mainly by water. Even though a lot of progress has been made regarding the completeness and accuracy of molecular line lists, the questions remains whether this is sufficient to achieve uncertainties for the metallicity below 0.10 dex. Towards colder stars the situation is

steadily worsening, and at around 2600 K grain formation becomes an important process. In the work presented in this thesis we have assumed that the spectra are not affected by magnetic fields or related activity. For the analyzed stars we argue that this is a valid assumption as we selected stars with low projected rotational velocities and mostly mid- to early spectral types. However, when expanding the analysis towards the later spectral types one may need to modify the analysis, coupled with additional observations to achieve knowledge of the magnetic field strength, as the activity level rises fast beyond mid-M dwarfs.

Another interesting way forward is to expand the wavelength range to have access to more atomic lines. With the old CRIRES spectrograph observations of the entire $J$ band were too time-consuming, but this is changing with the next generation of high-resolution infrared spectrographs. An estimate from the VALD database predicts 100 useful, unblended atomic lines in the $J$ band region for a M4 dwarf. This would enable to determine the abundance of several individual elements as well as a determination of the [$\alpha$/Fe] ratio. The larger amount of lines may also open up the possibility to determine $T_{\rm eff}$ and $\log g$ from spectral analysis and not have to be relying on external calibrations. This type of observations are already possible with currently operating spectrographs such as CARMENES, GIANO and iShell, and with future spectrographs like CRIRES$^+$ at the VLT and SPIRou at CFHT.

# 9. Contributions to the included papers

## Paper I

**Lindgren, S.**, Heiter, U. and Seifahrt, A. (2016)
*Metallicity determination of M dwarfs - High-resolution IR spectroscopy*
A&A, **597**, A100

The project was suggested by Ulrike Heiter, who had written the successful observing proposal. A former PhD student at the department, Anna Önehag, had reduced and analyzed the wide binaries and the individual M dwarfs (Önehag et al. 2012). Andreas Seifahrt provided me with individual spectra of the components in the close binaries. I continuum- and wavelength corrected the spectra. I re-did the adjustment of the line list and determined the metallicity of all binary components and the individual M dwarfs because of the adjustments of the line list and effective temperature. I conceived, developed, and tested the method to make use of the FeH lines to determine the effective temperature. I led the writing of all sections in the paper with input from Ulrike Heiter and Bengt Edvardsson, with the exception of Section 4.1 that was written by Andreas Seifahrt.

## Paper II

**Lindgren, S.** and Heiter, U. (2017)
*Metallicity determination of M dwarfs - Expanded parameter range in metallicity and effective temperature*
A&A, **604**, A97

The project was suggested by Ulrike Heiter. I ran the ESO pipeline and applied the additional wavelength- and continuum corrections for all the observational data. I performed the determination of the stellar parameters. I led the writing of all sections of the paper, with input from Ulrike Heiter.

# Paper III

**Lindgren, S.**, Heiter, U., Edvardsson, B., and Liljegren, S. (2017)
*A photometric calibration of M dwarfs based on high-resolution infrared spectroscopy*
To be submitted to A&A

The project was commonly agreed between Ulrike Heiter and myself. In collaboration with Sofie Liljegren I wrote the program to find the coefficients. I tested which magnitudes and colors that correlated with the metallicity. I collected the needed photometry and parallaxes for all used samples, where Ulrike Heiter helped with the collection of the photometry for the binaries included in the calibration sample. Bengt Edvardsson calculated the synthetic spectra and theoretical iso-metallicity curves, with the use of stellar evolution models provided to us by Greg Feiden. Sofie Liljegren determined the used statistical tests, and I determined the different validation tests. I led the writing of most sections of the paper, with input from coauthors. Bengt wrote the Section 3.2. and Sofie wrote parts of Sections 3.3 and 5.

# 10. Svensk sammanfattning

M-dvärgar är den vanligaste typen av stjärnor i vårt universum, och utgör ungefär 70% av alla stjärnor på sen så-kallade huvudserien. De är också de ljussvagaste och kallaste, med massor och radier 40-90% mindre än solens. Deras kalla yttemperatur ger upphov till ett spektrum som är dominerat av molekylära linjer.

Dessa små och kalla stjärnor har under de senaste åren blivit alltmer populära inom exoplanetsforskning, d.v.s. forskning som syftar till att upptäcka och karakterisera planeter kring andra stjärnor än vår egen sol. Att inkludera M-dvärgar i denna forskning är fördelaktigt av många anledningar. 1) Jämfört med sol-lika större stjärnor är det teknologiskt lättare att upptäcka jordstora planeter kring M-dvärgar. 2) Det är även mer sannolikt att hitta planeter som befinner sig i den beboeliga zonen, vilket är den region kring en stjärna där vatten förekommer i flytande form. 3) Vidare är omloppstiden för en planet i den beboeliga zonen betydligt kortare för en M-dvärg, vilket utgör en stor fördel för transitspektroskopi. 4) Slutligen är M-dvärgar intressanta för att testa och vidareutveckla teorin för planetbildning då deras låga massa tänjer på gränsen för hur effektiv planetbildningen måste vara för att det skall kunna bildas gasjättar som Jupiter.

Historiskt har det molekyldominerade spektrumet från M-dvärgar gjort att varken dess effektivtemperatur, ytgravitation eller grundämnessammansättning kunnat bestämmas med tillräckligt hög noggrannhet. De molekyler som bildas i atmosfären leder till miljontals absorptionslinjer där det optiska våglängdsområdet, vilket majoriteten av alla spektrografer är anpassade för, är speciellt påverkat. Eftersom linjedata för många molekyler är otillräcklig kan dessa linjer sällan användas. Vidare överlappar den stora mängden molekylära linjer de relativt mycket färre atomära linjerna, och försvårar därigenom analys av atomära linjer. Tidigare studier av M-dvärgar har därför förlitat sig på olika empiriska relationer mellan stjärnans luminositet och dess massa, radie, effektivtemperatur, ytgravitation eller metallhalt. Med metallhalt menas mängden av alla grundämnen förutom väte och helium, relativt mängden som uppmätts i solen.

Den första delen av denna avhandling behandlar en alternativ metod för att bestämma metallhalten hos M-dvärgar. Genom att istället för att observera M-dvärgar i det optiska, där deras spektra är helt dominerade av molekylära linjer, observerade vi dem i ett specifikt våglängdsintervall i det infraröda mellan 1100-1400 nm. Detta våglängdsområde är mindre påverkat av molekyler och individuella atomära absorptionslinjer och kontinuumnivån kan särskilja.

Tack vare detta kan metallhalten bestämmas genom att anpassa ett teoretiskt beräknat spektrum till ett tjugotal linjer, en metod som ger högre noggrannhet än empiriska relationer. För att verifiera att metoden ger pålitliga resultat analyserade vi ett antal M-dvärgar i dubbelstjärnesystem med en varmare sol-lik stjärna. De två stjärnorna har bildats från samma stoftmoln och förväntas därför ha samma metallhalt. Eftersom man kan bestämma metallhalten hos varmare stjärnor med hög noggrannhet, tack vare deras mindre komplexa spektrum, kan de användas för att kontrollera resultaten från M-dvärgarna. Vi använde denna metod för att analysera drygt 30 M-dvärgar med olika metallhalt och effektivtemperatur. Vi kunde sedan jämföra resultaten för de olika stjärnorna med vad vi får från olika empiriska relationer, och således uppskatta deras noggrannhet. Alla relationerna hade en relativt stor spridning och för majoriteten av stjärnorna gav de empiriska relationer ett längre värde för metallhalten än det vi fick från spektralanalysen.

Den andra delen av avhandlingen handlar om att ta fram en förbättrad empirisk relation eftersom de som fanns jämförde sig relativt dåligt med resultaten från spektralanalys. Empiriska fotometriska relationer bygger på att en stjärnas metallhalt kan bestämmas som en polynomfunktion av dess absolutmagnitud och färg. Vi använde oss av olika statistiska tester för att bestämma den optimala graden på polynomet. Koefficienterna bestämdes med hjälp av de 30-tal M-dvärgarna vi analyserat, tillsammans med några få väl utvalda M-dvärgar i dubbelstjärnor. Vår nya empiriska relation har mindre spridning jämfört med föregående fotometriska relationer, och ger jämförbara resultat för metallhalten av individuella stjärnor som spektroskopiska relationer.

Med hjälp av denna nya empiriska relation har vi kunnat visa att M-dvärgar som har minst en Jupiter-stor planet överlag har högre metallhalt än solen. Om vi jämför detta med metallhalten hos M-dvärgar med enbart små planeter finner vi däremot inte någon trend. Detta samband mellan jätteplaneter och metallhalt har redan påvisats för varmare stjärnor, vilket ledde till utvecklingen av den nuvarande planetbildningsteorin.

Framtiden ser ljus ut för M-dvärgar. Det pågår flera intressanta projekt som letar planeter kring M-dvärgar så som CARMENES, MEarth och TESS. Vidare satsar flera observatorier på instrument i det infraröda, t.ex. James Webb Space telescope, CRIRES$^+$, SPIRou och iSHELL. De tre sistnämnda erbjuder alla högupplösta spektrum liknade de vi använde i spektralanalysen av de 30 M-dvärgarna. Detta ger framtida forskare goda möjligheter att karakterisera M-dvärgar både med och utan planeter med hjälp av bland annat de metoder som presenteras i denna avhandling och göra nya spännande upptäckter för dessa kalla, små stjärnor.

# 11. Acknowledgements

First of all I would like to thank my supervisors Ulrike Heiter and Bengt Edvardsson for all suggestions and help along the way, and for allowing me to travel the world to meet new people and learn about new exciting, cool things in astronomy. I would also like to thank the rest of the people in the astronomy department in Uppsala for these years, where a specially thanks goes to all my fellow PhD students that have become my good friends over the years. I have enjoyed our time together both at Ångströms and outside the office with countless coffee breaks, board game nights, quiz, hikes and drinks.

To Naum for always being yourself and being someone I know I can always trust. To Sofie and Lisa for being the best office mates I could wish for, and for all fun we have experience over the years that hopefully will continue to do for a long time onwards. And thank you Sofie for making me take vacation at least once a year and go skiing, was well needed and always great fun. To Thomas for being the great guy you are and thanks all advises you given both about work and cats over the years. And last but not least, to James, Christian and Alexis for all being the nice guys you are and giving the department such a nice atmosphere. I would also like to thank my friends outside the department; Linda, Anna, Tim, Emily, Estelle, Lorena, Chris, Iulia, Pablo and many many more.

Lastly I would like to thank my family. I would not be here today and be the person I am without my parents Carl-Henrik and Annette, and my sister Ylva. I know you always have my back and supported me no matter what. Lastly I would like to show my deepest gratitude to Jonathan. Since we first meet you have always been there for me. Through this PhD we have shared a lot frustration and sleepless nights, but also a lot wonderful memories. I'm looking forward to the next chapter together with my favorite teammate.

# 12. References


Adibekyan, V. Z., Santos, N. C., Sousa, S. G., et al. 2012, A&A, 543, A89
Alibert, Y., Mordasini, C., & Benz, W. 2011, A&A, 526, A63
Allard, F. & Freytag, B. 2010, Highlights of Astronomy, 15, 756
Allard, F., Homeier, D., & Freytag, B. 2013, Mem. Soc. Astron. Italiana, 84, 1053
Asplund, M. 2005, ARA&A, 43, 481
Baraffe, I., Chabrier, G., Allard, F., & Hauschildt, P. H. 1998, A&A, 337, 403
Bean, J. L., Benedict, G. F., & Endl, M. 2006a, ApJ, 653, L65
Bean, J. L., Sneden, C., Hauschildt, P. H., Johns-Krull, C. M., & Benedict, G. F. 2006b, ApJ, 652, 1604
Benedict, G. F., Henry, T. J., Franz, O. G., et al. 2016, AJ, 152, 141
Bochanski, J. J., Hawley, S. L., Covey, K. R., et al. 2010, AJ, 139, 2679
Bodaghee, A., Santos, N. C., Israelian, G., & Mayor, M. 2003, A&A, 404, 715
Bonfils, X., Delfosse, X., Udry, S., et al. 2005, A&A, 442, 635
Breiman, L. & Spector, P. 1989, Submodel Selection and Evaluation in Regression: The X-random Case, Technical report (University of California, Berkeley. Department of Statistics) (Statistics Department, University of California)
Buchhave, L. A., Latham, D. W., Johansen, A., et al. 2012, Nature, 486, 375
Burnham, K. P. & Anderson, D. R. 2004, Sociological methods & research, 33, 261
Casagrande, L., Flynn, C., & Bessell, M. 2008, MNRAS, 389, 585
Castelli, F. & Kurucz, R. L. 2004, ArXiv Astrophysics e-prints
Covey, K. R., Hawley, S. L., Bochanski, J. J., et al. 2008, AJ, 136, 1778
Cumming, A., Marcy, G. W., & Butler, R. P. 1999, ApJ, 526, 890
Delfosse, X., Forveille, T., Ségransan, D., et al. 2000, A&A, 364, 217
Dressing, C. D. & Charbonneau, D. 2013, ApJ, 767, 95
Dressing, C. D. & Charbonneau, D. 2015, ApJ, 807, 45
Endl, M., Cochran, W. D., Kürster, M., et al. 2006, ApJ, 649, 436
Fischer, D. A. & Valenti, J. 2005, ApJ, 622, 1102
Gaidos, E. & Mann, A. W. 2014, ApJ, 791, 54
Gonzalez, G. 1997, MNRAS, 285, 403
Gonzalez, G., Carlson, M. K., & Tobin, R. W. 2010, MNRAS, 403, 1368
Gonzalez, G. & Laws, C. 2007, MNRAS, 378, 1141
Gray, D. F. 2005, The Observation and Analysis of Stellar Photospheres (Cambridge, UK: Cambridge University Press)
Gustafsson, B., Edvardsson, B., Eriksson, K., et al. 2008, A&A, 486, 951
Haisch, Jr., K. E., Lada, E. A., & Lada, C. J. 2001, ApJ, 553, L153
Hauschildt, P. H., Allard, F., Alexander, D. R., & Baron, E. 1997, ApJ, 488, 428
Hauschildt, P. H. & Baron, E. 1999, Journal of Computational and Applied Mathematics, 109, 41
Heiter, U. & Luck, R. E. 2003, AJ, 126, 2015
Hillenbrand, L. A. 2008, Physica Scripta Volume T, 130, 014024

Holmberg, J., Nordström, B., & Andersen, J. 2009, A&A, 501, 941
Ida, S. & Lin, D. N. C. 2004a, ApJ, 604, 388
Ida, S. & Lin, D. N. C. 2004b, ApJ, 616, 567
Ida, S. & Lin, D. N. C. 2005, ApJ, 626, 1045
Johns-Krull, C. M. & Valenti, J. A. 1996, ApJ, 459, L95
Johnson, J. A., Aller, K. M., Howard, A. W., & Crepp, J. R. 2010, PASP, 122, 905
Johnson, J. A. & Apps, K. 2009, ApJ, 699, 933
Kaeufl, H.-U., Ballester, P., Biereichel, P., et al. 2004, in Society of Photo-Optical Instrumentation Engineers (SPIE) Conference Series, Vol. 5492, Ground-based Instrumentation for Astronomy, ed. A. F. M. Moorwood & M. Iye, 1218–1227
Kornet, K., Bodenheimer, P., Różyczka, M., & Stepinski, T. F. 2005, A&A, 430, 1133
Laughlin, G. & Adams, F. C. 1997, ApJ, 491, L51
Lépine, S., Hilton, E. J., Mann, A. W., et al. 2013, AJ, 145, 102
Lindgren, S. & Heiter, U. 2017, A&A, 604, A97
Lindgren, S., Heiter, U., & Seifahrt, A. 2016, A&A, 586, A100
Luck, R. E. & Heiter, U. 2006, AJ, 131, 3069
Mann, A. W., Brewer, J. M., Gaidos, E., Lépine, S., & Hilton, E. J. 2013, AJ, 145, 52
Mann, A. W., Deacon, N. R., Gaidos, E., et al. 2014, AJ, 147, 160
Mann, A. W., Feiden, G. A., Gaidos, E., Boyajian, T., & von Braun, K. 2015, ApJ, 804, 64
Mayor, M. & Queloz, D. 1995, Nature, 378, 355
Mordasini, C., Alibert, Y., Benz, W., & Naef, D. 2008, in Astronomical Society of the Pacific Conference Series, Vol. 398, Extreme Solar Systems, ed. D. Fischer, F. A. Rasio, S. E. Thorsett, & A. Wolszczan, 235
Mulders, G. D., Pascucci, I., & Apai, D. 2015, ApJ, 798, 112
Neves, V., Bonfils, X., Santos, N. C., et al. 2012, A&A, 538, A25
Newton, E. R., Charbonneau, D., Irwin, J., et al. 2014, AJ, 147, 20
Nordström, B., Mayor, M., Andersen, J., et al. 2004, A&A, 418, 989
Nutzman, P. & Charbonneau, D. 2008, PASP, 120, 317
Önehag, A., Heiter, U., Gustafsson, B., et al. 2012, A&A, 542, A33
Pepe, F., Molaro, P., Cristiani, S., et al. 2014, Astronomische Nachrichten, 335, 8
Pinsonneault, M. H., DePoy, D. L., & Coffee, M. 2001, ApJ, 556, L59
Piskunov, N. & Valenti, J. A. 2017, A&A, 597, A16
Pollack, J. B., Hubickyj, O., Bodenheimer, P., et al. 1996, Icarus, 124, 62
Quirrenbach, A., Amado, P. J., Caballero, J. A., et al. 2014, in Society of Photo-Optical Instrumentation Engineers (SPIE) Conference Series, Vol. 9147, Society of Photo-Optical Instrumentation Engineers (SPIE) Conference Series, 1
Ribas, Á., Merín, B., Bouy, H., & Maud, L. T. 2014, A&A, 561, A54
Rojas-Ayala, B., Covey, K. R., Muirhead, P. S., & Lloyd, J. P. 2010, ApJ, 720, L113
Rojas-Ayala, B., Covey, K. R., Muirhead, P. S., & Lloyd, J. P. 2012, ApJ, 748, 93
Rosenblatt, F. 1971, Icarus, 14, 71
Santos, N. C., Israelian, G., & Mayor, M. 2001, A&A, 373, 1019
Santos, N. C., Israelian, G., Mayor, M., et al. 2005, A&A, 437, 1127
Schlaufman, K. C. & Laughlin, G. 2010, A&A, 519, A105
Seager, S. & Mallén-Ornelas, G. 2003, ApJ, 585, 1038
Shulyak, D., Reiners, A., Wende, S., et al. 2010, A&A, 523, A37

Sousa, S. G., Santos, N. C., Israelian, G., Mayor, M., & Udry, S. 2011, A&A, 533, A141
Sousa, S. G., Santos, N. C., Mayor, M., et al. 2008, A&A, 487, 373
Struve, O. 1952, The Observatory, 72, 199
Takeda, Y., Ohkubo, M., Sato, B., Kambe, E., & Sadakane, K. 2005, PASJ, 57, 27
Takeda, Y., Sato, B., Kambe, E., et al. 2001, PASJ, 53, 1211
Tennyson, J., Yurchenko, S. N., Al-Refaie, A. F., et al. 2016, Journal of Molecular Spectroscopy, 327, 73
Terrien, R. C., Mahadevan, S., Bender, C. F., et al. 2012, ApJ, 747, L38
Udry, S., Mayor, M., Benz, W., et al. 2006, A&A, 447, 361
Valenti, J. A. & Fischer, D. A. 2005, ApJS, 159, 141
Valenti, J. A. & Piskunov, N. 1996, A&AS, 118, 595
Valenti, J. A., Piskunov, N., & Johns-Krull, C. M. 1998, ApJ, 498, 851
Ward-Duong, K., Patience, J., De Rosa, R. J., et al. 2015, MNRAS, 449, 2618
West, A. A., Hawley, S. L., Walkowicz, L. M., et al. 2004, AJ, 128, 426
Woolf, V. M., Lépine, S., & Wallerstein, G. 2009, PASP, 121, 117
Woolf, V. M. & Wallerstein, G. 2005, MNRAS, 356, 963

Acta Universitatis Upsaliensis

*Digital Comprehensive Summaries of Uppsala Dissertations from the Faculty of Science and Technology* 1587

Editor: The Dean of the Faculty of Science and Technology

A doctoral dissertation from the Faculty of Science and Technology, Uppsala University, is usually a summary of a number of papers. A few copies of the complete dissertation are kept at major Swedish research libraries, while the summary alone is distributed internationally through the series Digital Comprehensive Summaries of Uppsala Dissertations from the Faculty of Science and Technology. (Prior to January, 2005, the series was published under the title "Comprehensive Summaries of Uppsala Dissertations from the Faculty of Science and Technology".)

Distribution: publications.uu.se
urn:nbn:se:uu:diva-332102

ACTA
UNIVERSITATIS
UPSALIENSIS
UPPSALA
2017